WARWICK
THE UNIVERSITY OF WARWICK

Manuscript version: Author's Accepted Manuscript
The version presented in WRAP is the author's accepted manuscript and may differ from the published version or Version of Record.

Persistent WRAP URL:
http://wrap.warwick.ac.uk/77556

How to cite:
Please refer to published version for the most recent bibliographic citation information.

Copyright and reuse:
The Warwick Research Archive Portal (WRAP) makes this work by researchers of the University of Warwick available open access under the following conditions.

Copyright © and all moral rights to the version of the paper presented here belong to the individual author(s) and/or other copyright owners. To the extent reasonable and practicable the material made available in WRAP has been checked for eligibility before being made available.

Copies of full items can be used for personal research or study, educational, or not-for-profit purposes without prior permission or charge. Provided that the authors, title and full bibliographic details are credited, a hyperlink and/or URL is given for the original metadata page and the content is not changed in any way.

Publisher's statement:
Please refer to the repository item page, publisher's statement section, for further information.

For more information, please contact the WRAP Team at: wrap@warwick.ac.uk.

warwick.ac.uk/lib-publications

Modeling of turn-OFF Transient Energy in IGBT Controlled Silicon PiN Diodes

Saeed Jahdi, *Mem. IEEE*, Olayiwola Alatise *Mem. IEEE* and Phil Mawby *Senior Mem. IEEE*
School of Engineering
University of Warwick
Coventry, CV4 7AL, United Kingdom
Phone: +44 (0) 2476151293
Fax: +44 (0) 2476418922
Email: S.Jahdi@warwick.ac.uk
URL: http://www2.warwick.ac.uk/fac/sci/eng/research/energyconversion/peater/

Keywords

<<PiN Diode>>, <<Reverse Recovery>>, <<Switching Energy>>, <<Modeling>>.

Abstract

Silicon PiN diodes are the most widely used rectifying technology in industry especially in voltage source converters. The PiN diodes are usually used as anti-parallel diodes across silicon IGBTs where they conduct current in the reverse direction as the current commutates between the phases of the converter. They tend to generate a considerable amount of energy losses during the turn-OFF transient due to the reverse recovery characteristics. The rate at which the diode is switched will determine the switching energy and will affect EMI, electrothermal stresses and reliability. Hence, it is vital to be able to predict the switching energy of the diode during its turn-OFF transient given the switching conditions so as to have a realistic approach towards predicting the operating temperature. The switching energy of PiN diodes is determined by the peak reverse recovery current, the peak diode voltage overshoot, the time displacement between them as well as the temperature dependency of these peaks. In this paper, a model is presented and validated over a temperature range of –75 °C to 175 °C and with switching speeds (*dI/dt*) modulated by the gate resistance on the low side IGBT ranging from 10 Ω to 1000 Ω. Comparisons show consistency between model prediction and measurements result. The model is a novel method of accurately predicting the switching energy of PiN diodes at different switching rates and temperatures using the measurements of a single switching rate at different temperatures.

Nomenclature

peak reverse recovery current at 25 °C	$I_{RR}^{(25\,^{\circ}C)}$	(A)
Forward Current	I_F	(A)
Diode Voltage 25 °C	$V_{AK}^{(25\,^{\circ}C)}$	(V)
Diode Current	i_D	(A)
Diode on-state Voltage Drop	V_D	(V)
turn-OFF Switching Rate	dI_{TF}/dt	(A/μ s)
Recovery switching Rate	dI_{RR}/dt	(A/μ s)
Voltage Recovery Rate	dV/dt	(V/μ s)
Switching Energy of the Diode	E_{SW}	(mJ)
Circuit Parasitic Inductance	L	(H)

Introduction

PiN diodes are the most widely used rectifying devices in power converters in industry [1]. They deliver low conduction losses because of conductivity modulation from minority carrier injection however they tend to have significant switching energy losses due to reverse recovery [2, 3]. The extraction of minority carriers in the voltage blocking drift layer during turn-OFF results in a large reverse current with a peak current and time duration that depends on the rate at which the PiN diode is switched off. These switching energy losses are considerable due to the overlap between the peak reverse recovery current and the peak

diode voltage overshoot [4] as shown in Figure 1(a). Conventional models used to predict this loss use simplistic equations which results in a degree of inaccuracy. This is shown in Figure 1(b).

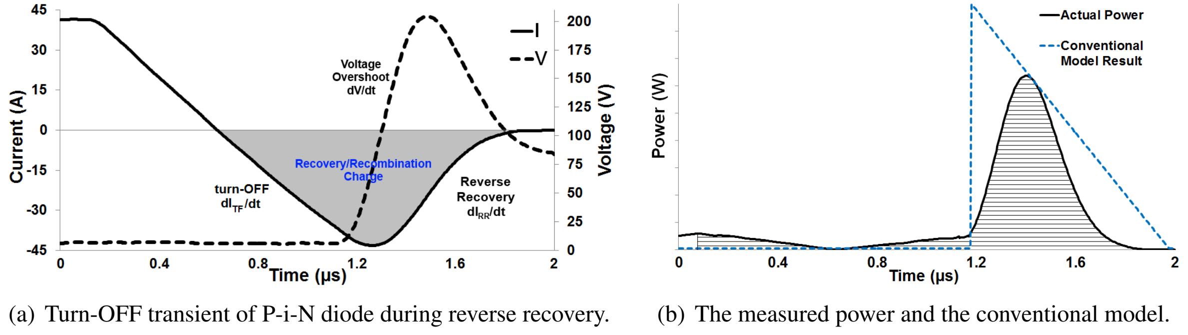

(a) Turn-OFF transient of P-i-N diode during reverse recovery.

(b) The measured power and the conventional model.

Figure 1: The Voltage, current and power behaviour during reverse recovery and its conventional modeling.

Equation (1) expresses the peak reverse recovery current (I_{RR}) as a function of the turn-OFF switching rate (dI_{TF}/dt), the derivation of which is shown in [5]. The peak reverse recovery current is known in to increase and the reverse recovery time is known to decrease as the turn-OFF switching rate increases. The reverse recovery characteristic also depends on the minority carrier lifetime, hence, lifetime treatment techniques can be used to reduce switching losses by reducing the reverse recovery charge [6]. In Equation (1), S is a measure of the softness of the diode's recovery characteristic (ratio of the time between the zero crossing of the current and the peak reverse current to the time between the peak of the current and the zero) and K_Q is a function that defines the relationship between the stored charge in the diode and the forward current (I_F) [7]. Snappy diodes are diodes that have very high dI/dt during the recovery phase of the turn-OFF characteristic where the current goes from the peak reverse current back to zero. This high dI/dt combined with parasitic inductances can cause significant voltage overshoots capable of causing device failure. Equation (2) accounts for the diode voltage (V_{AK}) plus the peak inductive voltage overshoot ($L\,dI_{TF}/dt$) resulting from the product of the switching rate and the parasitic inductance of the diode (L). Equation (3) is the switching energy of the diode (E_{SW}) expressed as a function of the peak reverse current, the peak diode voltage and the switching time i.e. the switching energy is calculated as the product of the peak voltage overshoot, the peak reverse recovery current and the total switching time. The total switching time is mathematically expressed as sum of the time required for the current to fall from the forward current to the peak reverse current (I_F+I_{RR}/ dI_{TF}/dt) and the time taken for the current to go from the peak reverse current back to zero (I_{RR}/ dI_{RR}/dt). K in (3) is the ratio of dI_{TF}/dt to dI_{RR}/dt.

$$I_{RR} = \sqrt{\frac{2k_Q\sqrt{I_F}}{1+S}}\sqrt{\frac{\mathrm{d}I_{TF}}{\mathrm{d}t}} \tag{1}$$

$$V_{AK} = V + L\frac{\mathrm{d}I_{TF}}{\mathrm{d}t} \tag{2}$$

$$\begin{aligned} E_{SW} &= \frac{1}{2}V_{AK}I_{RR}t_{SW} \\ &= \frac{1}{2}\left(\sqrt{\frac{2k_Q\sqrt{I_F}}{1+S}}\sqrt{\frac{\mathrm{d}I_{RR}}{\mathrm{d}t}}\right)\left(V+L\frac{\mathrm{d}I_{TF}}{\mathrm{d}t}\right)\left(\frac{I_F+I_{RR}}{K\frac{\mathrm{d}I_{TF}}{\mathrm{d}t}}\right) \\ &= \frac{1}{2}\left(\sqrt{\frac{2k_Q\sqrt{I_F}}{1+S}}\left(I_F+I_{RR}\left(1+\frac{1}{K}\right)\right)\right)\left(\frac{V}{\sqrt{\frac{\mathrm{d}I_{TF}}{\mathrm{d}t}}}+L\sqrt{\frac{\mathrm{d}I_{TF}}{\mathrm{d}t}}\right) \end{aligned} \tag{3}$$

In the next section, an accurate analytical model for calculating the switching energy of PiN diodes during reverse recovery in the turn-OFF transient is presented. The model uses measurements at a single switching rate and different temperatures to accurately predict the switching energy of the PiN diodes over a wide variety of switching rates. It is based on linearized approximations of current and voltage waveforms and incorporates the dependency of the peak voltage overshoot and reverse recovery current on the switching rate (dI/dt), accounts for the impact of temperature on the snappiness of the diodes

reverse recovery characteristics and the time displacement between the peak reverse recovery current and peak voltage overshoot [8]. The model is not a device-physics based model that requires detailed information of the device's physical geometry and processing parameters usually not available on the datasheet. Rather, the model is based on mathematical models of switching waveforms that have been extrapolated to cover different switching conditions. Although not as accurate as physics-based models, the advantage of this model is that the switching energy can be determined for any switching rate given some initial characterisation. The input parameters required for using the model are the desired voltage and current switching rates ($A/\mu s$ and $V/\mu s$), the forward and peak reverse recovery currents at a given temperature as well as the terminal supply voltage. The temperature dependencies of these parameters have also been taken into account. The model is validated through experimental measurements in a clamped inductive test rig at different temperatures and different *dI/dt* (modulated through a range of gate resistances). The results of the model are consistent with measurement results with as shown in model validation section. Using the equations developed in this paper, applications engineers can calculate the switching energy of the diode at a given temperature and switching rate using parameters extracted from initial measurements and other datasheet parameters.

Model Development

Figure 2 shows the linearized switching waveforms of the diode current and voltages including the reverse recovery and voltage overshoot. The instantaneous power is calculated by simply multiplying the voltage and current transients as shown in Figure 2 and the switching energy is calculated by integrating the switching power over time. The current and voltage transients shown in Figure 2 have been divided into different sections, where each section is characterized by a change in the transient waveform. Between t_1 and t_2, the current through the diode is ramping down at a defined and constant rate that depends on the gate resistance and input capacitance of the bottom side switching transistor. During this phase, the diode voltage remains constant at the on-state voltage which depends on the diodes on-state resistance. At time t_2, the diode current reaches zero and becomes negative while the diode voltage remains constant at its on-state value. Between time t_2 and t_3, the diode current continues on its negative ramp with a fixed slope. At time t_3, the diode voltage starts to increase as the electric field forms at the junctions. The increase of the diode voltage will depend on the rate of discharge of the internal diode capacitance formed in the depletion region. As the depletion regions form at the junctions of the PiN diode, the device becomes incapable of supporting the current through it, so the negative current reaches its peak (which is marked by time t_4) and the remaining minority carriers in the drift region start recombining. Between time t_4 and time t_5, the diode recombination current continues its positive ramp back to zero while the diode voltage reaches its peak value which depends on the supply voltage and the peak inductive overshoot. At time t_5, the diode voltage reaches its peak and at time t_6, the diode current reaches zero. The switching power plot shown in Figure 2 can be divided into distinct areas corresponding to the different switching phases. The total switching energy will be the sum of all the switching energies as shown in equation (4). Equations (5) and (6) respectively show the derived switching energies E_{SW1} and E_{SW2} corresponding to the current switching phase where the diode voltage is constant. The calculated switching energy corresponding to other sections of the switching transient can be calculated by equation (7) where the limits of the integration will depend on the section being integrated. The limits of the integration are shown in equation (8) for t_1 to t_6. The coefficients of the integration in equation (7) also depend on the section of the switching power transient being integrated. Equation (9) shows derived expressions for the coefficients corresponding to E_{SW3}, equation (10) for E_{SW4} and equation (11) for E_{SW5}.

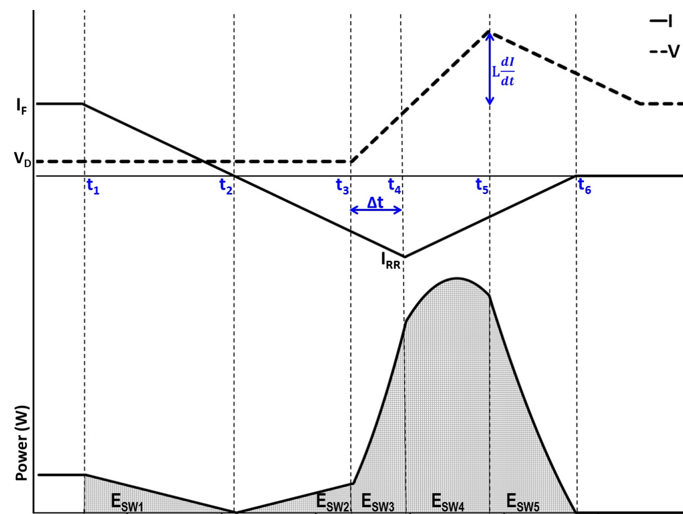

Figure 2: Power areas of the complete model valid for all *dI/dt* rates.

The total switching energy can be calculated using the equation below:

$$E_{SW} = \int_{t_1}^{t_2} V_{AK}(t) i_D(t) dt$$

$$E_{SW} = |E_{SW_1}| + |E_{SW_2}| + \sum_{n=3}^{5} |E_{SW_n}| \tag{4}$$

$$E_{SW_1} = \frac{I_F^2 V_D}{2\left(\frac{\mathrm{d}I_{TF}}{\mathrm{d}t}\right)} \tag{5}$$

$$E_{SW_2} = \frac{V_D}{2}\left(I_{RR} - \Delta t \frac{\mathrm{d}I_{RR}}{\mathrm{d}t}\right)\left(\frac{I_{RR}}{\frac{\mathrm{d}I_{RR}}{\mathrm{d}t}} - \Delta t\right) \tag{6}$$

$$E_{SW_n} = \frac{a_n b_n}{3}\left(t_{n+1}^3 - t_n^3\right) + \frac{a_n d_n + b_n c_n}{2}\left(t_{n+1}^2 - t_n^2\right) + b_n d_n \left(t_{n+1} - t_n\right) \tag{7}$$

The switching time intervals defined in Figure 2 can be calculated as:

$$t_1 = 0 \;,\; t_2 = \frac{I_F}{\frac{\mathrm{d}I_{TF}}{\mathrm{d}t}} \;,\; t_3 = \frac{I_F + I_{RR}}{\frac{\mathrm{d}I_{TF}}{\mathrm{d}t}} - \Delta t$$

$$t_4 = \frac{I_F + I_{RR}}{\frac{\mathrm{d}I_{TF}}{\mathrm{d}t}} \;,\; t_5 = \frac{I_F + I_{RR}}{\frac{\mathrm{d}I_{TF}}{\mathrm{d}t}} - \Delta t + \frac{V + \left(L\frac{\mathrm{d}I_{TF}}{\mathrm{d}t}\right) - V_D}{\frac{\mathrm{d}V}{\mathrm{d}t}} \;,\; t_6 = \frac{I_F + I_{RR}}{\frac{\mathrm{d}I_{TF}}{\mathrm{d}t}} + \frac{I_{RR}}{\frac{\mathrm{d}I_{RR}}{\mathrm{d}t}} \tag{8}$$

and the equation coefficients can be calculated as:

$$a_3 = -\frac{\mathrm{d}I_{TF}}{\mathrm{d}t} \;,\; b_3 = I_F \;,\; c_3 = \frac{\mathrm{d}V}{\mathrm{d}t} \;,\; d_3 = V_D - \frac{\mathrm{d}V}{\mathrm{d}t}\left(\frac{I_F + I_{RR}}{\frac{\mathrm{d}I_{TF}}{\mathrm{d}t}} - \Delta t\right) \tag{9}$$

$$a_4 = \frac{\mathrm{d}V}{\mathrm{d}t} \;,\; b_4 = V_D - \frac{\mathrm{d}V}{\mathrm{d}t}\left(\frac{I_F + I_{RR}}{\frac{\mathrm{d}I_{TF}}{\mathrm{d}t}} - \Delta t\right) \;,\; c_4 = \frac{\mathrm{d}I_{RR}}{\mathrm{d}t} \;,\; d_4 = -\frac{\mathrm{d}I_{RR}}{\mathrm{d}t}\left(\frac{I_F + I_{RR}}{\frac{\mathrm{d}I_{TF}}{\mathrm{d}t}} + \frac{I_{RR}}{\frac{\mathrm{d}I_{RR}}{\mathrm{d}t}}\right) \tag{10}$$

$$a_5 = \frac{\mathrm{d}I_{RR}}{\mathrm{d}t} \;,\; b_5 = -\frac{\mathrm{d}I_{RR}}{\mathrm{d}t}\left(\frac{I_F + I_{RR}}{\frac{\mathrm{d}I_{TF}}{\mathrm{d}t}} + \frac{I_{RR}}{\frac{\mathrm{d}I_{RR}}{\mathrm{d}t}}\right) \;,\; c_5 = \frac{\mathrm{d}V'}{\mathrm{d}t} = -\frac{\mathrm{d}V}{2\mathrm{d}t} \;,$$

$$d_5 = V + L\frac{\mathrm{d}I_{TF}}{\mathrm{d}t} + \frac{\mathrm{d}V}{2\mathrm{d}t}\left(\frac{I_F + I_{RR}}{\frac{\mathrm{d}I_{RR}}{\mathrm{d}t}} + \frac{V + \left(L\frac{\mathrm{d}I_{TF}}{\mathrm{d}t}\right) - V_D}{\frac{\mathrm{d}V}{\mathrm{d}t}} - \Delta t\right) \tag{11}$$

To ensure the temperature dependency of the switching energy is taken into account, the following temperature dependencies of the peak reverse current, peak diode overshoot and the switching rate have been incorporated into the model:

$$I_{RR} = I_{RR}^{(25°C)} + \frac{\mathrm{d}I_{TF}}{\mathrm{d}T}(T-25) \tag{12}$$

$$\frac{\mathrm{d}I_{RR}}{\mathrm{d}t} = \frac{\mathrm{d}I_{RR}}{\mathrm{d}t}^{(25°C)} - \frac{\mathrm{d}^2\mathrm{I_{RR}}}{\mathrm{d}t\mathrm{d}T}(T-25) \tag{13}$$

$$V_{AK} = V^{(25°C)} - \frac{\mathrm{d}V}{\mathrm{d}T}(T-25) \tag{14}$$

The peak reverse recovery current increases with temperature as a result of increased carrier lifetime resulting in higher reverse recovery charge. The rate of change of the peak reverse recovery current with temperature (dI_{RR}/dT) is extracted from reverse recovery measurements taken at different temperatures and is incorporated into the model in the form of equation (12). In equation (12), I_{RR} is the peak reverse recovery current at a given temperature and $I_{RR}(25\ °C)$ is the peak reverse recovery current at 25 °C. The rate of change of the turn of current through the diode is known to decrease with increasing temperature. This is due to the low side silicon IGBT which exhibits a slower turn-ON switching speed as the temperature is increased as a result of reduced carrier mobility. This temperature effect is incorporated into the model through equation (13) where the room temperature (25 °C) switching rate (dI_{RR}/dt) is used as an input parameter. The rate of change of the switching rate with temperature ($d^2I_{RR}/dtdT$) is also extracted for a given switching rate at different temperature. The peak diode voltage reached during the switching transient is the sum of the supply voltage and the inductive overshoot that depends on the switching rate and the parasitic inductance. This diode peak voltage (V_{AK}) reduces as the temperature increases because the switching rate of the low side IGBT reduces with increasing temperature for reasons explained earlier. This is incorporated into the model through equation (13) where the dV/dT is the rate of change of the peak diode voltage with temperature. The following section on the experimental measurements will show how all of these parameters have been extracted.

Experimental Measurements

To validate the model, the experimental measurements have been performed using a double-pulsed clamped inductive quasi switching test rig with a set-up shown below [9, 10]. Figure 3 shows the circuit schematic and Figure 4 shows a picture of the test rig. The test rig is equipped with a thermal chamber capable of varying the temperature within a range of –75 °C to 175 °C and the gate resistance on the gate driver of the test rig can be changed to any required resistance. In the case of these measurements, the gate resistance is varied between 10 Ω and 1000 Ω to vary the switching rate of the PiN diode (*dI/dt*). The initial gate pulse duration is set to 20 μs and the energizing pulse is set to 250 μs.

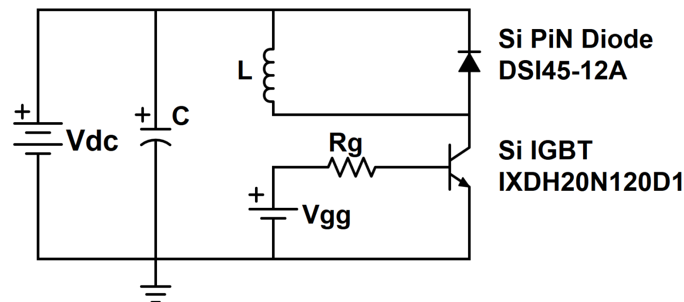

Figure 3: The schematic of the test rig design.

The value of the energizing inductance is 7.4 mH and the DC link capacitance is 940 μF. The gate voltage is set to 18 Volts. The measurements are done at a voltage rating of 100 V and 40 A, the current probe is degaussed within a range of 20 mV/A and the differential voltage probes are calibrated on a ratio of 1/100 V.

Figure 4: The Inductive clamped Measurement Test Rig including: 1- Environmental Chamber, 2- Signal Generator, 3- Oscilloscope, 4- Main power supply, 5- Interlock power supply, 6- 5V gate driver supply, 7- 18V gate driver supply, 8- capacitors, 9- Inductors, 10- Gate Driver, 11- Probe Amplifier, 12- Safety Volt meter.

Figure 5 shows the diode turn-OFF switching rate (dI_{CE}/dt) as a function of the gate resistance at different temperatures. It can be seen that the switching rate decreases as the gate resistance increases as is expected since increasing the gate resistance increases the electrical time constant. It can also be seen that increasing the ambient temperature reduces the switching rate as a result of increased minority carrier lifetime and decreased diffusivity i.e. charge formation in the drift region occurs at a slower rate. Figure 6 shows the turn-ON switching rate as a function of the gate resistance and temperature where it can be seen that the diode switching rate reduces with increasing R_G and temperature as expected.

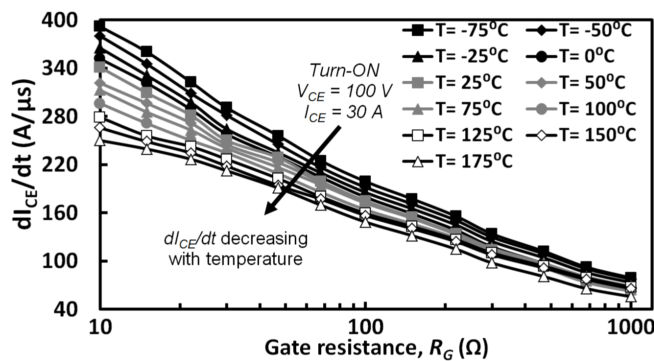

(a) *dI/dt* as a function of R_G

Figure 5: *dI/dt* on turn-ON of the IGBT as a function of temperature and gate resistance.

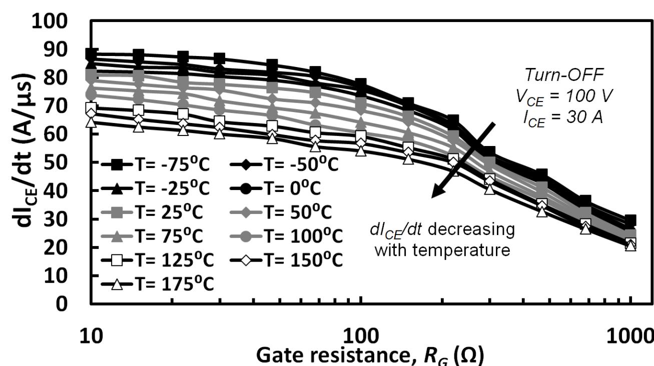

(a) *dI/dt* as a function of R_G

Figure 6: *dI/dt* on turn-OFF of the IGBT as a function of temperature and gate resistance.

Figure 7 shows the measured temperature dependencies of the peak reverse recovery current and the peak diode voltage overshoot for a given switching rate. Figure 7 shows that an increase in temperature results in an increase in the peak reverse recovery current and a decrease in the peak voltage overshoot of the device. These measurements as used to parameterize equations (12) and (14). The rate of change of the peak reverse recovery current is extracted and fed into equation (12) and the rate of change of the peak voltage overshoot with respect to temperature is fed into equation (14).

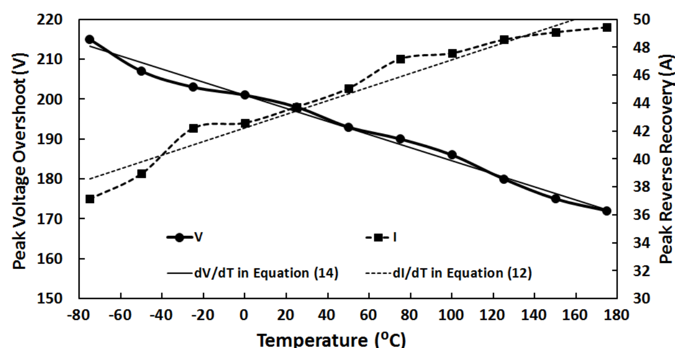

Figure 7: Temperature dependencies of the peak reverse recovery current and the peak diode voltage overshoot.

Figure 8(a), (b) and (c) shows the impact of temperature on the snappiness of the diodes reverse recovery at 3 different temperatures. The square symbols represent the measured *dI/dt* of the diode turn-OFF current when the carriers are being extracted in the opposite direction to conventional current flow i.e. the negative slope current between the zero crossing and the peak reverse recovery current which is between t_2 and t_4 in Figure 2. In this paper, this is referred to as the recovery phase in the turn-OFF current since the carriers are recovered. The line in Figure 8 represents the measured *dI/dt* between the peak reverse recovery current and zero which is between t_4 and t_6 in Figure. 2 i.e. the positive sloping current that is formed by minority carrier recombination in the charge storage region when the diode is in blocking mode and depletion regions have been formed at the junctions. In this paper, this is referred to as the recombination phase of the turn-OFF current. The maximum slope is extracted from the measurements in the 2 phases of reverse recovery. Diode snappiness can be defined as the ratio of the duration of the minority carrier extraction phase and minority carrier recombination phase. In Figure 2, this would be $(t_4 - t_2)/(t_6 - t_4)$ [5]. Diode snappiness can also be defined as the ratio of the *dI/dt* during carrier extraction and the *dI/dt* during carrier recombination [11, 12]. The diode is said to be snappy when the measured *dI/dt* during the recombination phase is higher than that in the recovery phase or the duration of the recombination phase is smaller than that during the recovery phase. Because excessively snappy diodes can cause reliability problems during hard commutation with high *dI/dt*, fabrication steps can be taken to ensure soft recovery. It can be seen from Figure 8 that at small gate resistances, the recombination *dI/dt* is higher than the recovery *dI/dt* and as the gate resistance is increased, the recombination *dI/dt* becomes smaller than the recovery *dI/dt*. It can also be seen from Figure 8 that the increase in temperature results in an increase in the snappiness of the diode. This is due to the fact that the increase in temperature has increased the *dI/dt* of the recombination slope while the reverse recovery slope has been decreased with temperature.

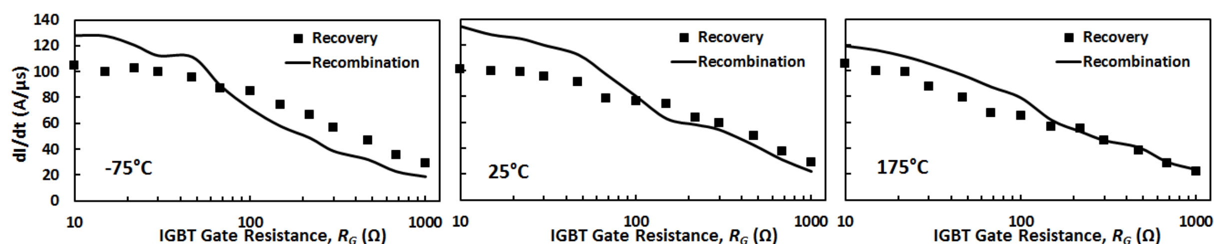

Figure 8: The ratio of Slopes of *dI/dt* on Recovery and Recombination varied by Temperature change.

Model Validation

Figure 9 shows the turn-ON and turn-OFF switching energy as functions of the switching rates and temperatures. As seen, the switching energy during diode turn-OFF is approximately 4 times higher than the turn-ON. This is mainly due to the reverse recovery phenomenon during the turn-OFF. The switching energy increases with temperature in both cases. The increase in switching energy during turn-ON is due to the fact that the *dI/dt* is decreasing with temperature as shown in Figure 5 which in turn results in slower transient and higher switching energy. The increase in switching energy during turn-OFF is

also due to the decrease in *dI/dt* and also an increase in the recovery charge due to increasing minority carrier lifetime with temperature. Therefore as seen in Figure 9(b), the increase in switching energy with temperature during turn-OFF is more significant. Figure 9 also shows that the switching energy reduces with reducing *dI/dt* initially before it starts increasing as the *dI/dt* is reduces further leading to a U-shaped characteristic. At high *dI/dt*, the high switching energy is due to high peak reverse recovery currents and high diode voltage overshoot, whereas at *dI/dt* the high switching energy is due to the long transient during the switching process. Therefore an optimum point exists where the switching energy is minimum.

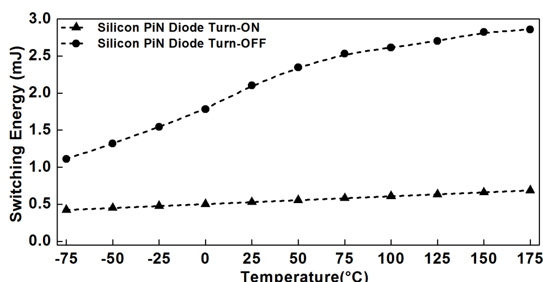

(a) As a Function of Temperature for R_G = 10 Ω

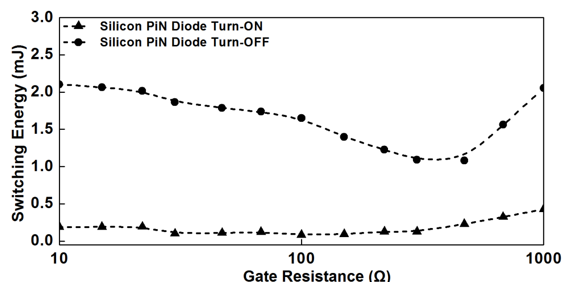

(b) As a Function of Gate Resistance at room Temperature

Figure 9: Experimental measurements of switching energy during turn-ON and turn-OFF of the Silicon PiN diode.

Figure 10 shows a comparison between the measurements and model at different (a) gate resistances and (b) different temperatures. As seen, the model has good estimation of the switching energy with a small error margin and is capable of predicting the trends with temperature and switching rates as well.

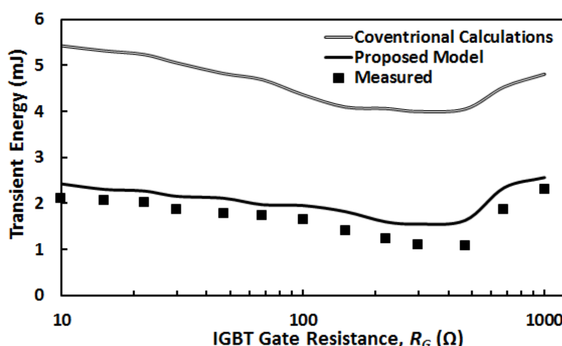

(a) Switching Energy as a function of R_G

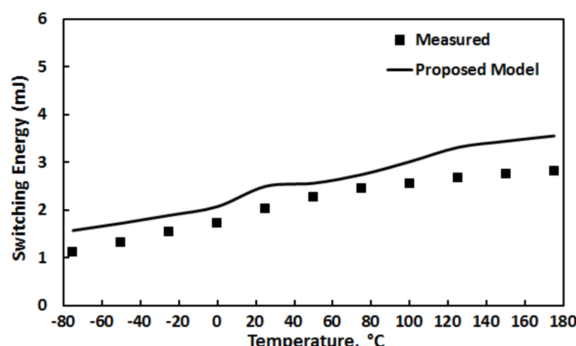

(b) Switching Energy as a function of temperature

Figure 10: Validation of the proposed model and comparison with measured switching energies.

Conclusion

PiN diodes normally exhibit a significant reverse recovery charge during the turn-OFF transient. This reverse charge is the cause of significant switching energy. This switching energy results in considerable temperature rise during turn-OFF, especially at higher switching frequencies. Since PiN diodes are still devices of choice in many applications, this energy requires accurate estimation. The switching energy exhibited by PiN diodes during turn-OFF also has a distinct temperature and switching rate dependency that can be modeled and extrapolated to different switching conditions. In this paper, an accurate analytical model for prediction of switching energy of PiN diodes during reverse recovery transient is presented. The model is based on waveform analytical modeling at different temperatures for a given switching rate and a subsequent extension of the waveform characteristics to different switching rates. The advantage of the model is that it does not rely on having information usually known only by manufacturers and standard datasheet parameters will suffice. The model is validated through extensive experimental measurements in a clamped inductive switching test rig. The model output has shown a good agreement with measurements results through a range of gate resistances and temperatures.

References

[1] Jahdi, S.; Alatise, O.; Fisher, C.; Ran, L.; Mawby, P., “An Evaluation of Silicon Carbide Unipolar Technologies for Electric Vehicle Drive-trains,” Emerging and Selected Topics in Power Electronics, IEEE Journal of, vol.PP, no.99, pp.1,1

[2] Bryant, A.T.; Liqing Lu; Santi, E.; Palmer, P.R.; Hudgins, J.L., “Physical Modeling of Fast p-i-n Diodes With Carrier Lifetime Zoning, Part I: Device Model,” Power Electronics, IEEE Transactions on , vol.23, no.1, pp.189,197, Jan. 2008

[3] Liqing Lu; Bryant, A.T.; Santi, E.; Palmer, P.R.; Hudgins, J.L., “Physical Modeling of Fast p-i-n Diodes With Carrier Lifetime Zoning, Part II: Parameter Extraction,” Power Electronics, IEEE Transactions on , vol.23, no.1, pp.198,205, Jan. 2008

[4] Yahaya, N.Z.; Khoo Choon Chew, “Comparative study of the switching energy losses between Si PiN and SiC Schottky diode,” Power and Energy Conference, 2004. PECon 2004. Proceedings. National, pp.216,219, 29-30 Nov. 2004

[5] Yueqing Wang; Qingyou Zhang; Jianping Ying; Chaoqun Sun, “Prediction of PIN diode reverse recovery,” Power Electronics Specialists Conference, 2004. PESC 04. 2004 IEEE 35th Annual, pp.2956-2959, Vol.4, 2004.

[6] Kao, Y.C.; Davis, J.R., “Correlations between reverse recovery time and lifetime of p-n junction driven by a current ramp,” Electron Devices, IEEE Transactions on , vol.17, no.9, pp.652,657, Sep 1970

[7] Al-Naseem, O.; Erickson, R.W.; Carlin, P., “Prediction of switching loss variations by averaged switch modeling,” Applied Power Electronics Conference and Exposition, 2000. APEC 2000. Fifteenth Annual IEEE, pp.242-248 vol.1, 2000.

[8] Jia, K.; WaŁrdemark, M.; Bohlin, G.; Thottappillil, R., ”Overshoot problem of the output diode used in the pre-charger for the railway propulsion system,” Power Electronics, IET , vol.5, no.7, pp.991,997, August 2012

[9] Jahdi, S.; Alatise, O.; Mawby, P.A., “The impact of silicon carbide technology on grid-connected Distributed Energy resources,” Innovative Smart Grid Technologies Europe (ISGT EUROPE), 2013 4th IEEE/PES, pp.1,5, 6-9 Oct. 2013

[10] Jahdi, Saeed; Alatise, Olayiwola; Mawby, Phil, “On the Performance of Voltage Source Converters based on Silicon Carbide Technology,” Telecommunications Energy Conference ‘Smart Power and Efficiency’ (INTELEC), Proceedings of 2013 35th International, pp.1,6, 13-17 Oct. 2013

[11] SEMIKRON Application Manual, “Operation principle of power semiconductors: Reverse recovery behaviour”, vol. 59, chapter 1.3.1.3, pages 42-43, 2012.

[12] Subhas chandra Bose, J.V. and Imrie, I. and Ostmann, H. and Ingram, P., “IXYS Semiconductor Application Manual”, SONIC A New Generation of Fast Recovery Diodes, pages 1-6.

[13] Bellone, S.; Della Corte, F.G.; Di Benedetto, L.; Licciardo, G.D., “An Analytical Model of the Switching Behavior of 4H-SiC p+-n-n+ Diodes from Arbitrary Injection Conditions,” Power Electronics, IEEE Transactions on, vol.27, no.3, pp.1641,1652, March 2012.

[14] Bellone, S.; Della Corte, F.G.; Albanese, L.F.; Pezzimenti, F., “An Analytical Model of the Forward IV Characteristics of 4H-SiC p-i-n Diodes Valid for a Wide Range of Temperature and Current,” Power Electronics, IEEE Transactions on, vol.26, no.10, pp.2835,2843, Oct. 2011.

[15] Chang, H. -R; Gupta, R.N.; Winterhalter, C.; Hanna, E., “Comparison of 1200 V silicon carbide Schottky diodes and silicon power diodes,” Energy Conversion Engineering Conference and Exhibit, 2000. (IECEC) 35th Intersociety, pp.174,179 vol.1, 2000.